The Astronomical Journal, 134:2046–2053, 2007 November


# *U*-BAND PHOTOMETRY OF KUIPER BELT OBJECTS

David Jewitt,[1,2] Nuno Peixinho,[1,3] and Henry H. Hsieh[1,2,4]
*Received 2007 July 29; accepted 2007 August 22*


## ABSTRACT

We present *U*-band photometry of Kuiper Belt objects taken to further investigate their color-orbit systematics. As at longer optical and near-infrared wavelengths, the *U*-band colors of Kuiper Belt objects show a wide range and a unimodal distribution. We find no evidence that color systematics in the Kuiper Belt are strongly wavelength-dependent. This observation is consistent with control of the reflection characteristics by a single (but unidentified) reddening material. No evidence is found for blue/ultraviolet absorption that can arise from charge transfer transitions in hydrated minerals in some primitive (C-type) asteroids. In the classical KBOs alone the $U - B$ and other color indices are most strongly correlated with the Tisserand parameter measured with respect to Neptune.


*Key words:* Kuiper Belt

## 1. INTRODUCTION

The Kuiper Belt is a thick disk of solar system bodies located beyond Neptune. It is thought to be a dynamically evolved relic of the Sun's protoplanetary disk. Kuiper Belt objects (KBOs) sustain peak surface temperatures ~40–50 K and may preserve primitive matter from the earliest epochs of the planetary system, including volatiles that are thermodynamically unstable in the hot, inner regions. Scientific interest in the nature of the Kuiper Belt is high, befitting its likely status as parent reservoir of the Jupiter family comets, as a tracer of early solar system processes, and as the closest example of a "debris disk."

Most known KBOs are so faint that physical measurements, other than of broadband optical magnitudes and colors, are precluded. The most secure results from broadband photometry are that (1) the optical and near-infrared colors of the KBOs are widely dispersed, with a range larger than for any other solar system population (Luu & Jewitt 1996; Jewitt & Luu 1998, 2001; Peixinho et al. 2004; Doressoundiram et al. 2005) and (2) that the colors are mutually correlated in the *BVRIJ* (0.45–1.2 $\mu$m) bands (Jewitt & Luu 1998; Davies et al. 2000; Hainaut & Delsanti 2002). The unexpectedly broad range of colors suggests a broad range of Kuiper Belt surface compositions, the origin of which is unknown. Early models invoked a competition between the effects of cosmic-ray bombardment and impact resurfacing (Luu & Jewitt 1996) or other processes (Delsanti et al. 2004) to produce the color diversity. Counterevidence (e.g., the lack of strong rotational color variations on individual KBOs and the lack of correlation between impact probabilities and colors) renders these explanations less likely (Jewitt & Luu 2001; Thébault & Doressoundiram 2003). Different colors could indicate widely different intrinsic compositions of the KBOs, but it is difficult to understand how compositional differences could arise given the low and nearly uniform temperatures existing across the observed portion of the Kuiper Belt. A significant fraction of the KBOs and their immediate progeny, the Centaurs, are coated in "ultrared matter" (URM) that is rare or absent on other small-body populations in the solar system (Jewitt 2002; Hainaut & Delsanti 2002). The identification of this material is uncertain, although there exists a widely held suspicion that irradiated, complex organics are responsible for the URM (Cruikshank et al. 2007).

Whereas color versus color correlations are strong in the *BVRI* filters, in general the colors are not well correlated with the dynamical parameters of the KBOs. One exception is that the $B - R$ colors of the classical KBOs (CKBOs) are reportedly related to the perihelion distance, $q$, such that objects with $q >$ 40 AU are predominantly red (Tegler & Romanishin 2000). However, the inclinations and perihelion distances are related, and the color versus perihelion relation has been recast as a color versus inclination relation by Trujillo & Brown (2002). They and others find that the $B - R$ color is inversely related to the inclination at the ~3 or 4 $\sigma$ level of confidence. Doressoundiram et al. (2005) report that the significance of the color-inclination trend is sensitive to the precise sample used to define the CKBOs. On the other hand, measurements of 72 KBOs in $V - I$ show no significant correlation with inclination (Stephens et al. 2003), leading these authors to suggest that part of the strength of the correlation lies in the shorter wavelengths (*B* filter). This possibility is interesting, given that many minerals of likely solar system relevance possess broad absorption bands in the blue and near ultraviolet portions of the spectrum (Feierberg et al. 1985).

The possibility that the color-orbit systematics of the KBOs might be associated with a blue/UV absorber motivated us to extend KBO photometric measurements to shorter wavelengths. In this paper we present *U*-band photometry of KBOs from Mauna Kea, taking advantage of the low atmospheric extinction at the 4200 m altitude of this mountain.

## 2. OBSERVATIONS

All observations were taken using the Keck I 10 m diameter telescope located atop Mauna Kea, Hawaii, and its Low Resolution Imaging Spectrometer (LRIS) camera (Oke et al. 1995). Light entering the LRIS camera is divided according to wavelength by a dichroic filter and sent into separate red and blue cameras having independent charge-coupled device (CCD) imagers.

[1] Institute for Astronomy, University of Hawaii, 2680 Woodlawn Drive, Honolulu, HI 96822, USA; jewitt@ifa.hawaii.edu, peixinho@ifa.hawaii.edu.
[2] Observer at the W. M. Keck Observatory, a scientific partnership among the California Institute of Technology, the University of California, and the National Aeronautics and Space Administration. The Observatory was made possible by the generous financial support of the W. M. Keck Foundation.
[3] Grupo de Astrofisica, Universidade de Coimbra, Coimbra, Portugal.
[4] Queen's University, Belfast, Northern Ireland; h.hsieh@qub.ac.uk.

TABLE 1
FILTERS

| Filter | $\lambda_c$[a] (Å) | FWHM[a] (Å) | $k_\lambda$[b] |
|---|---|---|---|
| *U* | 3450 | 525 | 0.45 |
| *B* | 4370 | 878 | 0.15 |
| *V* | 5473 | 948 | 0.12 |
| *R* | 6417 | 1269 | 0.09 |
| *I* | 8331 | 3131 | 0.06 |

[a] Central wavelength and FWHM are computed for a white-light source and will be slightly different for real KBOs.
[b] Representative extinction coefficient measured for each filter.

This arrangement conveys a doubling of the observational efficiency relative to single-channel instruments. We used the "460" dichroic (which has 50% transmission at 4874 Å) to send short wavelengths to a blue-side CCD having $4096 \times 4096$ pixels, each 0.135 arcsec$^2$. The blue side of LRIS was used to record images in the *U* and *B* filters. Images through *V*, *R*, and *I* filters were recorded using the red-side detector having $2048 \times 2048$ pixels each 0.215 arcsec$^2$. The approximate central wavelengths and full widths at half-maximum (FWHMs) of the filters are listed in Table 1.

To calibrate the images we recorded bias frames and a set of flat-field images using an artificial light to illuminate the inside of the Keck dome. While the *V* and *R* filter dome flats were found to be of high quality, we determined that *U* and *I* filter flats computed from median combinations of the night-sky data were superior to the dome flats. In both cases, this can be plausibly attributed to differences between the spectrum of the dome flat-field lamps and the night sky itself. Photometric calibration was obtained using the faintest standard stars from the list by Landolt (1992), including Markarian A3, PG 2213−006C, PG 1323−085C, 92-249, and PG 1047+003B. These stars have high photometric accuracy ($1\ \sigma < 0.01$ mag.) and colors close to those of the Sun, thereby minimizing color correction terms in the calibration. The standards were further observed close to the air masses of the target KBOs, in order to minimize the extinction corrections. We used the standard stars to determine extinction coefficients on each night: representative values are given in Table 1. Given typical air-mass differences $\sim$0.1, the extinction corrections for all filters other than *U* were small compared to the uncertainties in the photometry. Even in the *U* filter, extinction corrections between the KBOs and the standards were only $\sim$0.04 mag or less, which is very small compared to the $\sim$0.6 mag dispersion in the $U - B$ colors of KBOs actually measured. Therefore, we are confident that the color differences measured among KBOs are not of instrumental or atmospheric origin. The CFHT Skyprobe (a small optical camera used to repeatedly measure the atmospheric transmission) was employed to assess the overall quality of each night. In addition, an up-looking 10 $\mu$m imager maintained by the Subaru Observatory on Mauna Kea provided additional information about thin cirrus. When clouds were seen or suspected, we pursued backup observational programs unrelated to the present work. Later measurements of the Landolt stars proved consistent at the $\pm$0.01 to $\pm$0.02 mag level except on UT 2007 February 20, when slightly larger fluctuations of unknown origin were occasionally observed.

Images were autoguided on field stars at sidereal rates using the Keck off-axis guider. The standard integration time was fixed near 300 s in order to keep the trailing motion of the KBOs relative to background stars $\leq 0.3''$. This is small compared to the seeing FWHM (typically $0.6''$–$1.0''$) and therefore of no consequence in the subsequent extraction of the photometry. We identified the KBOs by their motions relative to the fixed stars and galaxies in successive images. Usually this was possible in real time by comparing consecutive images from the Keck but, for those very slow objects near their turning points, we used images taken at the University of Hawaii 2.2 m telescope on other nights to confirm the identities of the KBOs.

We rejected from the sample some objects which appeared projected close to background stars and galaxies. For the remainder, we used aperture photometry to measure the magnitudes. We used both simple photometry with a fixed large diameter aperture (typically $4''$) and aperture correction (in which field stars are used to estimate the fraction of the light within an aperture, typically $2''$ diameter, that would otherwise be too small to permit reliable photometry). In all cases the most challenging measurements were those taken through the *U* filter because of the reduced sensitivity of the LRIS CCD. For the brighter targets ($U < 21$) the two methods gave comparable results. For fainter KBOs the method of aperture correction proved superior because of the reduced impact of uncertainties in the background sky.

TABLE 2
JOURNAL OF OBSERVATIONS

| Object | UT Date | $r$[a] (AU) | $\Delta$[b] (AU) | $\alpha$[c] (deg) |
|---|---|---|---|---|
| 86047 (1999 OY3) | 2003 Aug 30 | 39.447 | 38.561 | 0.70 |
| 44594 (1999 OX3) | 2003 Sep 22 | 25.674 | 24.986 | 1.65 |
| 55636 (2002 TX300) | 2003 Sep 22 | 40.838 | 39.916 | 0.57 |
| | 2004 Oct 10 | 40.954 | 40.020 | 0.50 |
| 2001 QX322 | 2003 Sep 22 | 39.354 | 38.476 | 0.72 |
| 2002 PP149 | 2003 Sep 22 | 38.605 | 37.658 | 0.49 |
| 26308 (1998 SM165) | 2003 Sep 22 | 35.646 | 34.709 | 0.59 |
| 55637 (2002 UX25) | 2003 Sep 22 | 42.557 | 41.657 | 0.61 |
| 24835 (1995 SM55) | 2003 Sep 22 | 39.139 | 38.320 | 0.86 |
| 55565 (2002 AW197) | 2004 Feb 16 | 47.149 | 46.192 | 0.30 |
| 40314 (1999 KR16) | 2004 Feb 16 | 37.165 | 36.770 | 1.40 |
| 82158 (2001 FP185) | 2004 Feb 16 | 34.251 | 33.487 | 1.06 |
| 42355 (2002 CR46) | 2004 Feb 17 | 17.697 | 16.727 | 0.62 |
| 2000 CN105 | 2004 Feb 17 | 46.066 | 45.084 | 0.14 |
| 82155 (2001 FZ173) | 2004 Feb 17 | 32.940 | 32.156 | 1.06 |
| 20000 Varuna | 2004 Feb 17 | 43.205 | 42.505 | 0.93 |
| 2000 CQ105 | 2004 Feb 17 | 49.514 | 48.538 | 0.18 |
| 82075 (2000 YW134) | 2004 Feb 17 | 43.176 | 42.295 | 0.60 |
| | 2007 Feb 20 | 43.648 | 42.761 | 0.57 |
| 65489 Ceto (2003 FX128) | 2004 Feb 17 | 25.866 | 25.305 | 1.83 |
| 2003 UZ117 | 2004 Feb 17 | 39.732 | 39.995 | 1.37 |
| | 2004 Oct 10 | 39.733 | 38.856 | 0.70 |
| 2001 QC298 | 2004 Oct 10 | 40.571 | 39.772 | 0.85 |
| 79360 (1997 CS29) | 2007 Feb 20 | 43.532 | 42.635 | 0.55 |
| 136472 (2005 FY9) | 2007 Feb 20 | 51.984 | 51.181 | 0.64 |
| 136108 (2003 EL61) | 2007 Feb 20 | 51.171 | 50.521 | 0.84 |
| 2003 GH55 | 2007 Feb 20 | 40.778 | 40.385 | 1.28 |

[a] Heliocentric distance.
[b] Geocentric distance.
[c] Phase angle.

## 3. OBSERVATIONAL RESULTS

A journal of observations, listed chronologically, is provided in Table 2. The orbital elements of the observed objects are listed for reference in Table 3, where they are ranked by

TABLE 3
Orbital Elements

| Object | $a$[a] (AU) | $e$[b] | $i$[c] (deg) | $q$[d] (AU) | $T_N$[e] | Class[f] |
|---|---|---|---|---|---|---|
| 2003 GH55 | 44.439 | 0.087 | 1.10 | 40.593 | 3.098 | CKBO |
| 79360 (1997 CS29) | 43.868 | 0.009 | 2.25 | 43.494 | 3.099 | CKBO |
| 42355 (2002 CR46) | 38.358 | 0.543 | 2.43 | 17.537 | 2.679 | nCKBO |
| 44594 (1999 OX3) | 32.188 | 0.456 | 2.63 | 17.518 | 2.774 | nCKBO |
| 2000 CN105 | 44.814 | 0.097 | 3.41 | 40.472 | 3.097 | CKBO |
| 82155 (2001 FZ173) | 86.699 | 0.626 | 12.71 | 32.423 | 2.930 | nCKBO |
| 26308 (1998 SM165) | 48.231 | 0.376 | 13.46 | 30.078 | 2.906 | nCKBO |
| 20000 Varuna | 43.224 | 0.056 | 17.14 | 40.790 | 2.984 | CKBO |
| 55637 (2002 UX25) | 42.820 | 0.145 | 19.42 | 36.614 | 2.929 | CKBO |
| 2000 CQ105 | 57.152 | 0.395 | 19.70 | 34.566 | 2.911 | nCKBO |
| 82075 (2000 YW134) | 58.479 | 0.296 | 19.76 | 41.168 | 3.021 | nCKBO |
| 65489 Ceto (2003 FX128) | 102.234 | 0.825 | 22.28 | 17.868 | 2.223 | nCKBO |
| (15874) 1996 TL66 | 84.904 | 0.587 | 23.94 | 35.040 | 2.840 | nCKBO |
| 86047 (1999 OY3) | 43.754 | 0.167 | 24.26 | 36.432 | 2.856 | CKBO |
| 55565 (2002 AW197) | 47.509 | 0.128 | 24.31 | 41.449 | 2.839 | CKBO |
| 40314 (1999 KR16) | 48.455 | 0.299 | 24.88 | 33.943 | 2.818 | nCKBO |
| 55636 (2002 TX300) | 43.511 | 0.124 | 25.86 | 38.118 | 2.905 | CKBO |
| 24835 (1995 SM55) | 42.151 | 0.108 | 26.96 | 37.580 | 2.812 | CKBO |
| 19308 (1996 TO66) | 43.597 | 0.116 | 27.33 | 38.533 | 2.815 | CKBO |
| 2003 UZ117 | 44.040 | 0.128 | 27.47 | 38.392 | 2.813 | CKBO |
| 136108 (2003 EL61) | 43.276 | 0.190 | 28.18 | 35.056 | 2.771 | CKBO |
| 2001 QX322 | 58.012 | 0.385 | 28.50 | 35.676 | 2.772 | nCKBO |
| 136472 (2005 FY9) | 45.758 | 0.154 | 29.00 | 38.693 | 2.789 | CKBO |
| 2001 QC298 | 46.155 | 0.121 | 30.63 | 40.556 | 2.768 | CKBO |
| 82158 (2001 FP185) | 221.811 | 0.846 | 30.78 | 34.254 | 2.624 | nCKBO |
| 2002 PP149 | 40.966 | 0.092 | 34.73 | 37.211 | 2.644 | CKBO |

[a] Semimajor axis.
[b] Orbital eccentricity.
[c] Orbital inclination.
[d] Perihelion distance.
[e] Tisserand parameter with respect to Neptune.
[f] CKBO = classical, nCKBO = nonclassical.

inclination $i$. Other quantities in Table 3 are the orbital semimajor axis $a$, eccentricity $e$, perihelion distance $q$, and Tisserand parameter relative to Neptune:

$$T_N = \frac{a_N}{a} + 2\left[\left(1 - e^2\right)\frac{a}{a_N}\right]^{1/2} \cos i. \quad (1)$$

In equation (1), $a_N = 30.07$ AU is the semimajor axis of Neptune's orbit. The Tisserand parameter is a constant of the motion in the restricted, circular three-body problem. Objects with $T_N > 3$ are more likely to be dynamically decoupled from Neptune than those with $T_N < 3$.

The photometry is summarized in Table 4. Measurements of objects observed on more than one night are listed separately in Table 4, along with the weighted averages of the different values. The photometric uncertainties listed in the table are the standard deviations on the means of independent measurements within each filter. Table 4 shows that the colors of a given object are generally reproducible to within the photometric uncertainties of a few percent. In addition, comparison of the colors from the present work with colors reported elsewhere shows generally good agreement. This indicates that rotational variations of the color must be small, as reported in previous studies (Luu & Jewitt 1996; Jewitt & Luu 2001; Doressoundiram et al. 2005). In Table 4 the absolute red magnitude of each object is computed from

$$R(1, 1, 0) = R - 5\log(r\Delta) - \beta\alpha, \quad (2)$$

in which $r$ and $\Delta$ are the heliocentric and geocentric distances in AU, $\alpha$ (deg) is the phase angle (see Table 2), and $\beta$ (mag deg$^2$) is the phase coefficient. We assumed $\beta = 0.04$ mag deg$^2$, similar to values measured on some large, icy KBOs (Sheppard & Jewitt 2002; Rabinowitz et al. 2007; Sheppard 2007). Larger $\beta$ values have been determined for some KBOs and might apply to the objects observed here. However, the maximum phase angles reached by the KBOs are $\alpha \sim 1^\circ$ (Table 2); the phase angle corrections are therefore small, and the adopted value of $\beta$ is not critical to our work.

Methods for the dynamical classification of KBOs continue to evolve. However, classification is complicated both by uncertainties in the orbital elements of the objects, caused by limited data, and by the fact that the distributions of many of the orbital elements are continuous, not discrete, so that unambiguous separations into groups cannot be made (Elliot et al. 2005). We employed a simplistic but practical scheme to classify the KBOs as either "classical" (CKBOs) or "nonclassical" (nCKBOs; Table 3). Specifically, objects with semimajor axes between the 3:2 and 2:1 resonances (at 39.3 and 47.6 AU, respectively) are referred to in our work as members of the classical population: all others (including resonant objects and scattered KBOs) are by definition nonclassical. Close examination shows that most nCKBOs in our sample are scattered KBOs (SKBOs), dynamically distinguished from the classicals by having repeated interactions with Neptune that have lead to the gradual excitation of their inclinations and eccentricities. In fact, recent work shows that the SKBOs spend up to half their lives

TABLE 4
PHOTOMETRY SUMMARY

| Object | Date | $i$[a] (deg) | $R$[b] | $R(1,1,0)$[c] | $U-B$ | $B-V$ | $V-R$ | $R-I$ |
|---|---|---|---|---|---|---|---|---|
| 2003 GH55 | 2007 Feb 20 | 1.1 | 22.03±0.05 | 5.90±0.05 | 0.49±0.11 | 1.12±0.05 | 0.63±0.06 | 1.16±0.06 |
| 79360 (1997 CS29) | 2007 Feb 20 | 2.2 | 21.28±0.01 | 4.92±0.01 | 0.73±0.06 | 1.09±0.08 | 0.67±0.08 | 0.67±0.04 |
| 42355 (2002 CR46) | 2004 Feb 17 | 2.4 | 19.55±0.01 | 7.17±0.01 | 0.21±0.03 | 0.74±0.02 | 0.52±0.01 | ... |
| 44594 (1999 OX3) | 2003 Sep 22 | 2.6 | 21.24±0.02 | 7.14±0.02 | 0.27±0.06 | 1.17±0.03 | 0.62±0.03 | ... |
| 2000 CN105 | 2004 Feb 17 | 3.4 | 21.80±0.01 | 5.21±0.01 | 0.56±0.09 | 1.10 ±0.02 | 0.66±0.02 | 0.64±0.02 |
| 82155 (2001 FZ173) | 2004 Feb 17 | 12.7 | 20.94±0.01 | 5.77±0.01 | 0.25±0.04 | 0.87±0.02 | 0.52±0.02 | 0.52±0.02 |
| 26308 (1998 SM165) | 2003 Sep 22 | 13.5 | 20.87±0.02 | 5.38±0.02 | 0.21±0.05 | 1.10±0.40 | 0.65±0.03 | ... |
| 20000 Varuna | 2004 Feb 17 | 17.2 | 19.93±0.01 | 3.57±0.01 | 0.42±0.02 | 0.85±0.02 | 0.64±0.02 | 0.62±0.02 |
| 55637 (2002 UX25) | 2003 Sep 22 | 19.5 | 19.74±0.02 | 3.47±0.02 | 0.26±0.05 | 0.98±0.05 | 0.54±0.03 | ... |
| 2000 CQ105 | 2004 Feb 17 | 19.6 | 22.83±0.02 | 5.92±0.02 | 0.29±0.09 | 0.67±0.01 | 0.44±0.01 | ... |
| 82075 (2000 YW134) | 2004 Feb 17 | 19.8 | 20.64±0.01 | 4.31±0.01 | 0.31±0.04 | 0.92±0.02 | 0.55±0.03 | ... |
| | 2007 Feb 20 | 19.8 | 20.75±0.03 | 4.37±0.03 | 0.45±0.17 | 0.97±0.07 | 0.52±0.03 | 0.53±0.05 |
| | Average of 2004 Feb 17 and 2007 Feb 20 | 19.8 | 20.65±0.01 | 4.32±0.01 | 0.32±0.04 | 0.92±0.02 | 0.54±0.02 | 0.53±0.05 |
| 65489 Ceto (2003 FX128) | 2004 Feb 17 | 22.3 | 20.38±0.01 | 6.23±0.01 | 0.23±0.04 | 0.86±0.03 | 0.56±0.03 | ... |
| 15874 (1996 TL66)[d] | 1997 Aug 27 | 23.9 | ... | 5.32±0.04 | 0.23±0.20 | 0.74±0.08 | 0.40±0.05 | 0.26±0.07 |
| 86047 (1999 OY3) | 2003 Aug 30 | 24.3 | 22.18±0.02 | 6.24±0.02 | 0.30±0.02 | 0.80±0.06 | 0.40±0.04 | ... |
| 55565 (2002 AW197) | 2004 Feb 16 | 24.3 | 19.75±0.02 | 3.05±0.02 | 0.32±0.03 | 0.89±0.02 | 0.58±0.02 | 0.60±0.02 |
| 40314 (1999 KR16) | 2004 Feb 16 | 24.9 | 21.32±0.02 | 5.59±0.02 | 0.44±0.10 | 1.21±0.05 | 0.67±0.04 | 0.74±0.03 |
| 55636 (2002 TX300) | 2003 Sep 22 | 25.8 | 19.25±0.02 | 3.17±0.02 | 0.14±0.02 | 0.70±0.02 | 0.32±0.02 | ... |
| | 2004 Oct 10 | 25.8 | 19.24±0.02 | 3.15±0.02 | 0.17±0.02 | 0.65±0.02 | 0.38±0.02 | 0.36±0.02 |
| | Average of 2003 Sep 22 and 2004 Oct 10 | 25.8 | 19.25±0.02 | 3.16±0.01 | 0.16±0.01 | 0.68±0.01 | 0.35±0.01 | 0.36±0.02 |
| 24835 (1995 SM55) | 2003 Sep 22 | 27.0 | 20.21±0.02 | 4.30±0.02 | 0.18±0.02 | 0.67±0.02 | 0.32±0.02 | ... |
| 19308 (1996 TO66)[d] | 1997 Aug 27 | 27.3 | ... | 4.52±0.05 | 0.28±0.14 | 0.72±0.07 | 0.40±0.04 | 0.38±0.04 |
| 2003 UZ117 | 2004 Feb 17 | 27.5 | 20.98±0.01 | 4.92±0.01 | 0.19±0.02 | 0.66±0.02 | 0.33±0.02 | 0.32±0.02 |
| | 2004 Oct 10 | 27.5 | 20.88±0.02 | 4.91±0.02 | 0.11±0.04 | 0.70±0.03 | 0.37±0.02 | 0.37±0.05 |
| | Average of 2004 Feb 17 and Oct 10 | 27.5 | 20.96±0.01 | 4.92±0.01 | 0.17±0.02 | 0.67±0.02 | 0.35±0.01 | 0.33±0.02 |
| 136108 (2003 EL61) | 2007 Feb 20 | 28.2 | 17.28±0.03 | 0.18±0.03 | 0.11±0.04 | 0.61±0.02 | 0.37±0.02 | 0.32±0.02 |
| 2001 QX322 | 2003 Sep 22 | 28.5 | 22.30±0.02 | 6.37±0.02 | 0.07±0.07 | 0.91±0.03 | 0.55±0.03 | ... |
| 136472 (2005 FY9) | 2007 Feb 20 | 29.0 | 16.77±0.03 | −0.38±0.03 | 0.29±0.04 | 0.87±0.02 | 0.46±0.02 | 0.29±0.02 |
| 2001 QC298 | 2004 Oct 10 | 30.6 | 22.46±0.03 | 6.39±0.03 | 0.16±0.12 | 0.75±0.08 | 0.49±0.03 | 0.48±0.04 |
| 82158 (2001 FP185) | 2004 Feb 16 | 30.8 | 21.28±0.03 | 5.94±0.03 | 0.33±0.07 | 0.86±0.04 | 0.52±0.04 | 0.55±0.04 |
| 2002 PP149 | 2003 Sep 22 | 34.8 | 23.07±0.03 | 7.24±0.03 | 0.10±0.13 | 0.85±0.10 | 0.28±0.04 | ... |

[a] Orbital inclination.
[b] Apparent red magnitude.
[c] Absolute red magnitude, computed from $R(1,1,0) = R - 5\log_{10}(r\Delta) - 0.04\alpha$.
[d] Color indices are from Barucci et al. (1999), who present no $R$-band magnitudes. The absolute $R$-band magnitudes are from Jewitt & Luu (1998).

temporarily trapped in weak mean-motion resonances with Neptune (Lykawka & Mukai 2007b). Some of the KBOs in our sample are indeed in or near mean-motion resonances (26308 in the 2:1, 82075 in the 8:3), but none of them belong to the 3:2 "Plutino" family. More elaborate dynamical classification schemes are beginning to appear (e.g., Lykawka & Mukai 2005, 2007a). However, the scheme adopted here has the advantage of simplicity, and the results we derived are, in any case, not materially changed by the adoption of more elaborate methods of orbital classification.

Spearman's nonparametric rank test was used to search for correlations in our data. We sought correlations among the color indices within each group and between the color indices and absolute magnitudes, taken to be a proxy for size. We also searched for correlations between the colors and the orbital inclination, eccentricity, semimajor axis, perihelion distance, aphelion distance, and Tisserand parameter. No significant correlations were found with eccentricity, semimajor axis, or aphelion distance. Results for these and other correlations are summarized in Tables 5 and 6. Error bars on the correlation coefficients were computed using 1000 bootstrap replications (Efron & Tibshirani 1993).

The strongest correlations with any dynamical property are found among the CKBOs. There, the correlations between color and Tisserand parameter $T_N$ exceed 3 $\sigma$ significance in $U-B$, $V-R$, $R-I$, and $U-R$ (Table 5). The color correlations with $T_N$ are slightly stronger than with $i$ or $q$ (see Table 5), but the difference is small, reflecting the small size of the observational sample. The observed correlation is qualitatively consistent with earlier reports that $B-R$ is correlated with $q$ (Tegler & Romanishin 2000) and/or with $i$ (Trujillo & Brown 2002), since $T_N$ is correlated with both (Table 5). The contrast with the nCKBOs, which show no statistically significant correlations (Table 6), is dramatic (compare Figs. 1 and 2).

The meaning of the color-orbit relation in the CKBOs (Fig. 1, Table 5) and its absence in the nCKBOs (Fig. 2; Table 6) remains obscure. In some models the former are assumed to be primordial red objects and the latter to be less red (more nearly spectrally neutral) objects that were scattered outwards from formation at smaller distances. These assumptions are based on

TABLE 5
CORRELATIONS: CKBOs

| Variables[a] | | $N$[b] | $\rho^{+\sigma}_{-\sigma}$[c] | Prob.[d] | Sigma[e] |
|---|---|---|---|---|---|
| $U-B$ | $B-V$ | 15 | $0.74^{+0.11}_{-0.19}$ | 0.0017 | 3.14 |
| $U-B$ | $V-R$ | 15 | $0.85^{+0.09}_{-0.14}$ | 0.00006 | 4.01 |
| $U-B$ | $R-I$ | 11 | $0.78^{+0.13}_{-0.23}$ | 0.0043 | 2.85 |
| $U-B$ | $B-R$ | 15 | $0.80^{+0.11}_{-0.17}$ | 0.00035 | 3.58 |
| $U-B$ | $R(1,1,0)$ | 15 | $0.03^{+0.32}_{-0.35}$ | 0.93 | 0.09 |
| $U-B$ | $q$ | 15 | $0.66^{+0.16}_{-0.22}$ | 0.0071 | 2.69 |
| $U-B$ | $i$ | 15 | $-0.83^{+0.15}_{-0.09}$ | 0.00014 | 3.81 |
| $U-B$ | $T_N$ | 15 | $0.86^{+0.08}_{-0.14}$ | 0.00004 | 4.10 |
| $B-V$ | $q$ | 15 | $0.57^{+0.17}_{-0.24}$ | 0.027 | 2.21 |
| $B-V$ | $i$ | 15 | $-0.63^{+0.23}_{-0.19}$ | 0.011 | 2.54 |
| $B-V$ | $T_N$ | 15 | $0.68^{+0.16}_{-0.22}$ | 0.0051 | 2.80 |
| $V-R$ | $q$ | 15 | $0.71^{+0.14}_{-0.18}$ | 0.0030 | 2.97 |
| $V-R$ | $i$ | 15 | $-0.72^{+0.21}_{-0.12}$ | 0.0023 | 3.05 |
| $V-R$ | $T_N$ | 15 | $0.77^{+0.13}_{-0.16}$ | 0.00075 | 3.37 |
| $R-I$ | $q$ | 11 | $0.77^{+0.09}_{-0.22}$ | 0.0053 | 2.79 |
| $R-I$ | $i$ | 11 | $-0.85^{+0.24}_{-0.12}$ | 0.00099 | 3.29 |
| $R-I$ | $T_N$ | 11 | $0.82^{+0.13}_{-0.22}$ | 0.0018 | 3.12 |
| $B-R$ | $q$ | 15 | $0.65^{+0.18}_{-0.24}$ | 0.0094 | 2.60 |
| $B-R$ | $i$ | 15 | $-0.69^{+0.22}_{-0.14}$ | 0.0042 | 2.86 |
| $B-R$ | $T_N$ | 15 | $0.75^{+0.13}_{-0.20}$ | 0.0014 | 3.19 |
| $U-R$ | $q$ | 15 | $0.70^{+0.14}_{-0.20}$ | 0.0036 | 2.91 |
| $U-R$ | $i$ | 15 | $-0.74^{+0.20}_{-0.12}$ | 0.0017 | 3.14 |
| $U-R$ | $T_N$ | 15 | $0.80^{+0.11}_{-0.16}$ | 0.00038 | 3.56 |
| $q$ | $i$ | 15 | $-0.43^{+0.30}_{-0.22}$ | 0.11 | 1.60 |
| $q$ | $T_N$ | 15 | $0.53^{+0.21}_{-0.26}$ | 0.044 | 2.01 |
| $i$ | $T_N$ | 15 | $-0.98^{+0.04}_{-0.01}$ | <0.00001 | >8.00 |

[a] Variables: $q$, perihelion (AU); $i$, orbital inclination (deg); $T_N$, Tisserand parameter with respect to Neptune.
[b] Number of elements.
[c] Spearman rank correlation coefficient with error bars.
[d] Probability of obtaining the measured $\rho$ by chance, given $N$, i.e., significance.
[e] Equivalent significance under a Gaussian probability distribution.

TABLE 6
CORRELATIONS: nCKBOs

| Variables[a] | | $N$[b] | $\rho^{+\sigma}_{-\sigma}$[c] | Prob.[d] | Sigma[e] |
|---|---|---|---|---|---|
| $U-B$ | $B-V$ | 11 | $0.21^{+0.36}_{-0.40}$ | 0.53 | 0.63 |
| $U-B$ | $V-R$ | 11 | $0.04^{+0.36}_{-0.35}$ | 0.90 | 0.12 |
| $U-B$ | $R-I$ | 4 | $1.00^{+0.00}_{-0.13}$ | 0.20 | 1.28 |
| $U-B$ | $B-R$ | 11 | $0.13^{+0.37}_{-0.37}$ | 0.71 | 0.38 |
| $U-B$ | $R(1,1,0)$ | 11 | $-0.33^{+0.34}_{-0.28}$ | 0.32 | 0.99 |
| $U-B$ | $q$ | 11 | $0.21^{+0.34}_{-0.43}$ | 0.53 | 0.63 |
| $U-B$ | $i$ | 11 | $0.26^{+0.40}_{-0.45}$ | 0.43 | 0.79 |
| $U-B$ | $T_N$ | 11 | $0.21^{+0.32}_{-0.37}$ | 0.53 | 0.63 |
| $B-V$ | $q$ | 11 | $-0.07^{+0.36}_{-0.37}$ | 0.83 | 0.21 |
| $B-V$ | $i$ | 11 | $0.03^{+0.34}_{-0.37}$ | 0.93 | 0.09 |
| $B-V$ | $T_N$ | 11 | $0.14^{+0.32}_{-0.35}$ | 0.68 | 0.41 |
| $V-R$ | $q$ | 11 | $-0.32^{+0.33}_{-0.26}$ | 0.34 | 0.96 |
| $V-R$ | $i$ | 11 | $0.01^{+0.31}_{-0.33}$ | 0.98 | 0.03 |
| $V-R$ | $T_N$ | 11 | $-0.17^{+0.33}_{-0.23}$ | 0.63 | 0.48 |
| $R-I$ | $q$ | 4 | $-0.40^{+0.75}_{-0.29}$ | 0.60 | 0.52 |
| $R-I$ | $i$ | 4 | $0.60^{+0.11}_{-0.33}$ | 0.40 | 0.84 |
| $R-I$ | $T_N$ | 4 | $-0.60^{+0.32}_{-0.12}$ | 0.40 | 0.84 |
| $B-R$ | $q$ | 11 | $-0.15^{+0.39}_{-0.38}$ | 0.66 | 0.44 |
| $B-R$ | $i$ | 11 | $0.04^{+0.35}_{-0.38}$ | 0.92 | 0.11 |
| $B-R$ | $T_N$ | 11 | $0.00^{+0.31}_{-0.31}$ | 0.99 | 0.01 |
| $U-R$ | $q$ | 11 | $-0.24^{+0.37}_{-0.34}$ | 0.48 | 0.70 |
| $U-R$ | $i$ | 11 | $0.02^{+0.36}_{-0.37}$ | 0.96 | 0.05 |
| $U-R$ | $T_N$ | 11 | $0.00^{+0.30}_{-0.28}$ | 1.0 | 0.00 |
| $q$ | $i$ | 11 | $0.64^{+0.20}_{-0.31}$ | 0.035 | 2.10 |
| $q$ | $T_N$ | 11 | $0.44^{+0.25}_{-0.31}$ | 0.18 | 1.34 |
| $i$ | $T_N$ | 11 | $-0.28^{+0.37}_{-0.34}$ | 0.40 | 0.84 |

[a] Variables: $q$, perihelion (AU); $i$, orbital inclination (deg); $T_N$, Tisserand parameter with respect to Neptune.
[b] Number of elements.
[c] Spearman rank correlation coefficient with error bars.
[d] Probability of obtaining the measured $\rho$ by chance, given $N$, i.e., significance.
[e] Equivalent significance under a Gaussian probability distribution.

(and therefore consistent with) the measured color systematics, and perhaps are consistent the color versus $T_N$ correlation as well, but they are also completely ad hoc (i.e., the question of *why* the CKBOs should be redder than the nCKBOs is unaddressed).

There is no correlation between the colors and the absolute magnitudes of the KBOs. However, the different color indices are correlated with each other. Objects which are red in the $U-B$ index are red in all the other optical color indices. In order to further explore these color versus color correlations we computed reflectivity spectra from the broadband colors by subtracting the colors of the Sun (we used $U-B=0.19$, $B-V=0.63$, $V-R=0.36$, and $R-I=0.33$; cf. Hardorp 1982; Tueg & Schmidt-Kaler 1982; Hartmann et al. 1990) and normalizing the data to unity at the $R$ band. The colors of the Sun are notoriously difficult to determine (Cayrel de Strobel 1996), but they are probably accurate to $\pm0.01$ or $\pm0.02$ mag, an error which is small compared to the photometric uncertainties on most of the KBOs (Table 4). The resulting reflectivity spectra are shown in Figures 3 and 4, in which vertical offsets have been added for clarity of presentation. These figures emphasize that the optical reflection spectra of KBOs are, to first order, linear with wavelength and have spectral gradients spread over a wide range, from neutral (e.g., 24835, 55636, and 15874) or even slightly blue relative to the Sun (e.g., 136108) to red (e.g., 2003 GH55, 1997 CS29, 40314).

Figures 3 and 4 provide no evidence for the existence of a pronounced blue/UV absorption of the type that is characteristic of certain main-belt asteroids broadly grouped into the "C-type" class. Blue/UV absorption is observed in some but not all low-albedo, compositionally primitive asteroids (particularly in the broadly defined "C-complex"). It is a defining feature of Tholen & Barucci's (1989) C and G spectral types. The blue/UV absorption is present in iron- and titanium-containing minerals, where it is due to overlapping series of charge transfer bands (Burns 1981). Among C-type asteroids, the $U-B$ color index is correlated with the strength of the 3 $\mu$m absorption band from water in hydrated minerals (see Fig. 2 of Feierberg et al. 1985). The same correlation is observed in carbonaceous chondrites, leading to the suggestion that $U-B$ might be useful as an indicator of the presence of phyllosilicates and other hydrated materials (Gaffey & McCord 1978).

Figure 5 shows a color-color plot of the new data. The color of the Sun is marked in the figure, as is a line showing the locus of colors expected if the reflectivity gradient is constant with respect to wavelength. Measured colors fall on this "reddening line" line or to its right, indicating that the reflectivity gradient in $U-B$ is, on average, smaller than in $B-R$, both for classical and nonclassical KBOs. A $U$-band absorber would cause the slope to steepen in $U-B$, dragging the points to the left of the reddening line and the opposite of what is observed in Figure 5. An observational selection effect against finding objects having large $U-B$ indices might be expected given the $U$-band limited nature of the data. However, the data show no statistically significant relation between $U-B$ and $U$.

Figure 6 compares the normalized reflectivity spectra of KBOs 136108, 2003 UZ117, and 15874 with the spectra of F,

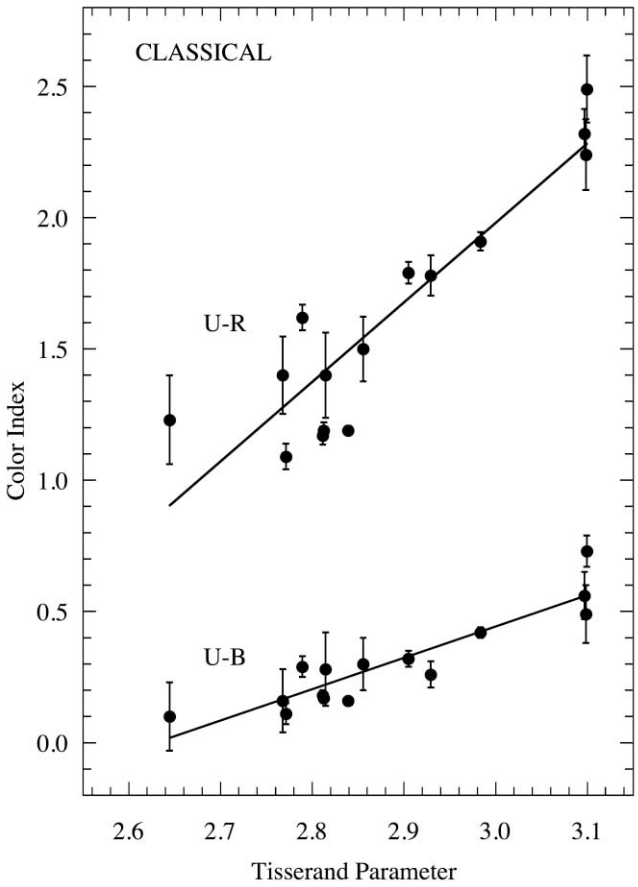


FIG. 1.—Color indices ($U - R$ at the top, $U - B$ at the bottom) vs. Tisserand parameter measured with respect to Neptune for CKBOs. Linear regression fits to the data are also shown. The correlations are significant at the 3.6 and 4.1 $\sigma$ levels in $U - R$ and $U - B$, respectively (Table 5).

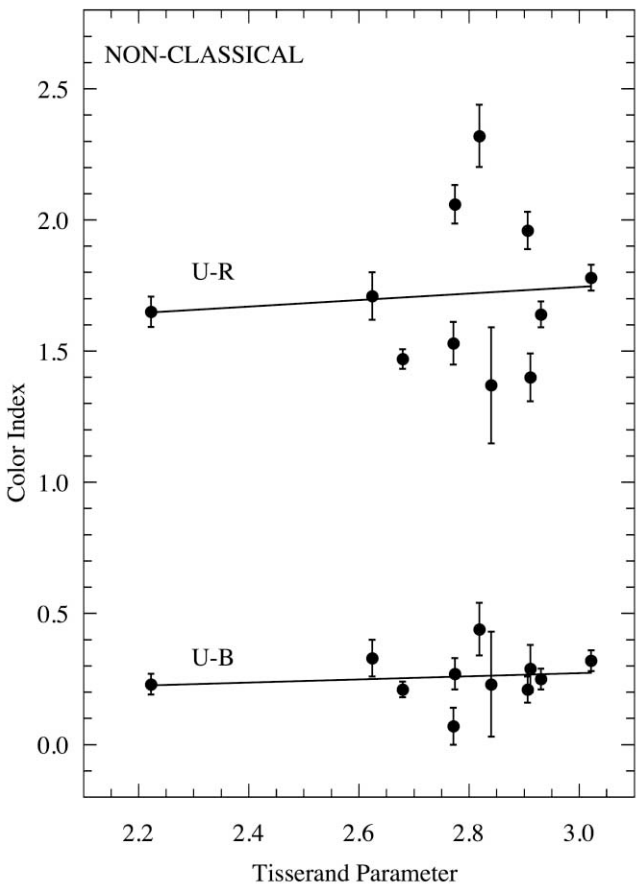


FIG. 2.—Color indices ($U - R$ at the top, $U - B$ at the bottom) vs. Tisserand parameter measured with respect to Neptune for nCKBOs. Linear regression fits to the data are also shown. Neither of the colors shows a significant correlation with $T_N$ (Table 6).

B, C, and G asteroids from the C-complex as defined by Tholen & Barucci (1989). The KBOs were selected to be the three in our sample most similar to C-complex asteroids in their overall optical spectral slope. The comparison shows no convincing evidence for the presence of a blue/UV absorber in these (or any other) KBOs (Fig. 6). One possible interpretation is that the surface materials on the KBOs are, and always have been, too far below the triple point (273 K) for liquid water to be sustained, precluding the possibility of aqueous alteration reactions that created the hydrated minerals on asteroids and in meteorites. Indeed, surface temperatures on the KBOs are near ~40–50 K, while evidence from the crystallinity of water ice requires only that the surface ices have been briefly heated to ~110 K since formation (Jewitt & Luu 2004). Tentative observational evidence has been produced attesting to the presence of hydrated minerals on KBOs, including bands near 1.4–2.25$\mu$m in Keck spectra of KBO 26375 (Jewitt & Luu 2001) and various optical bands in the 6000–8000 Å wavelength range in 47932 and (38628) Huya (de Bergh et al. 2004). Unfortunately, we have failed to repeat our own detections of the infrared bands in 26375 with better spectra from the Subaru telescope, and we are unaware of any observational confirmation of the optical features in 47932 and 38628. Thermal models allow liquid water, and the possibility for aqueous alteration reactions, in the interiors of middle and large-sized KBOs (Busarev et al. 2003; Merk & Prialnik 2006). However, compelling evidence for the presence of hydrated minerals on the surfaces of KBOs may fairly be said to be lacking.

Another, perhaps more direct possibility is that the blue/UV absorber is absent simply because the surface materials are unrelated to those in the main belt. Reflectivity spectra that are featureless from the near-UV to the near-IR, as are the KBOs, are produced in complex, carbon-bearing materials like oil-sand, coal, and coal-tar extract (Cloutis et al. 1994). These materials also tend to show concave-up reflection spectra consistent with some of the KBOs shown in Figures 3 and 4. Many complex organic compounds furthermore have low optical albedos like those of nonicy KBOs. Unfortunately, the absence of distinct absorption features in the spectra renders the identification of such materials a highly intractable task.

## 4. SUMMARY

The main results from this study are

1. The $U - B$ colors of the classical Kuiper Belt objects are most strongly correlated with $T_N$, the Tisserand parameter measured with respect to Neptune.

2. The $U - B$ colors are statistically correlated with other optical colors in the visible wavelength range (consistent with a single reddening agent). They are not correlated with the absolute magnitude (which we take as a proxy for the object size). Featureless optical spectra are a characteristic of some complex organic solids, but a unique identification cannot be made.

3. No evidence for a blue/UV ($\lambda < 5000$ Å) absorber is detected in the reflection spectra of KBOs. In asteroids and

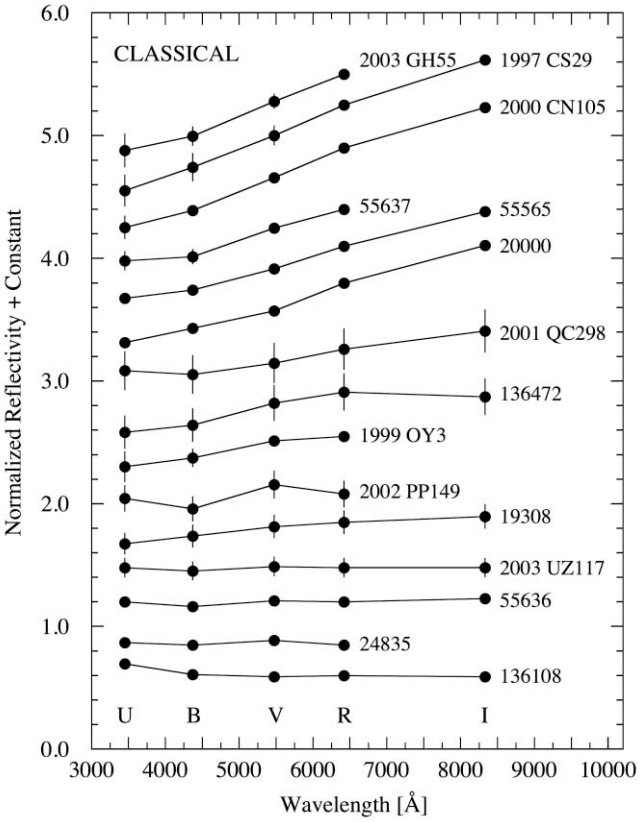


FIG. 3.—Reflectivity spectra of the CKBOs computed from the broadband photometry in Table 4. The spectra have been normalized at the *R* band, but are vertically offset for clarity of presentation.

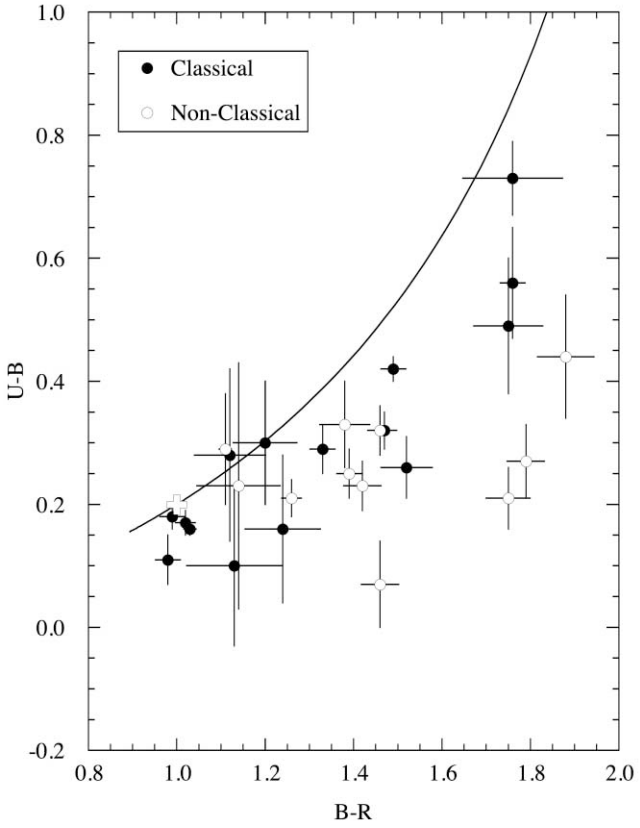


FIG. 5.—$U - B$ vs. $B - R$ color-color plot for the classical ( *filled circles*) and nonclassical (*open circles*) KBOs. The solid line shows the trajectory of reflectivity spectra having constant spectral gradient. The color of the Sun is plotted with an open plus sign.

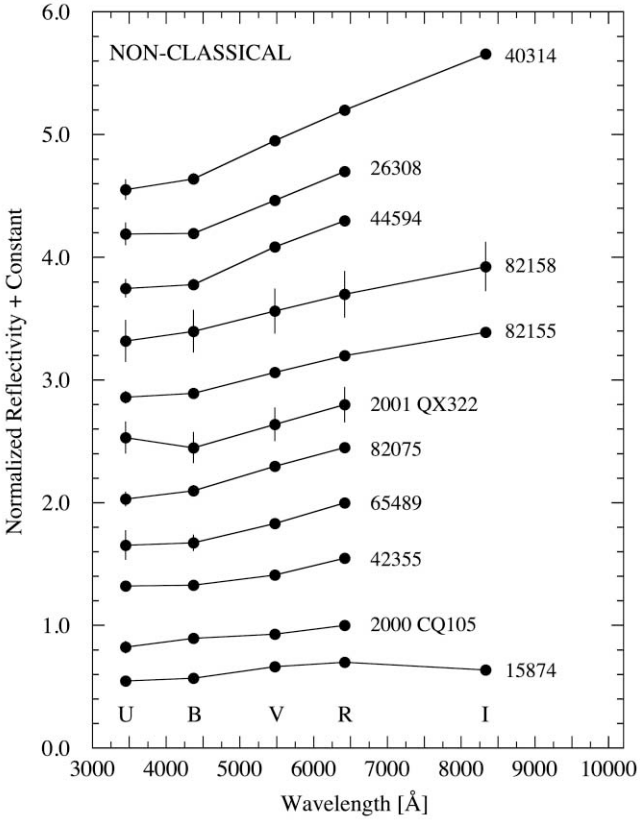


FIG. 4.—Reflectivity spectra of the nonclassical KBOs computed from the broadband photometry in Table 4. The spectra have been normalized at the *R* band, but are vertically offset for clarity of presentation.

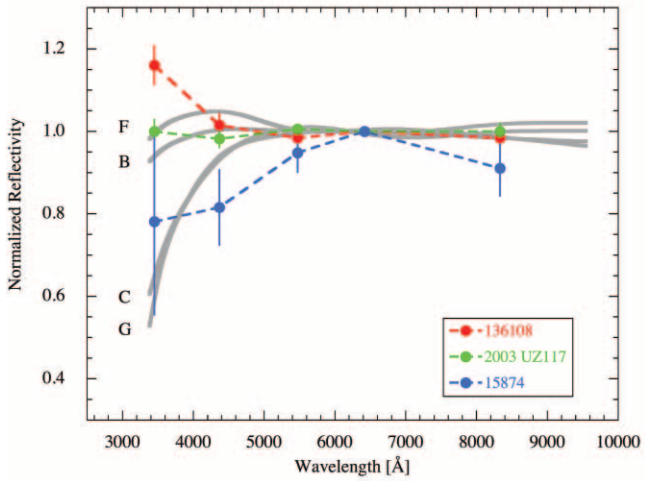


FIG. 6.—Normalized reflection spectra of three blue/neutral KBOs (*colored symbols*) compared with the F, B, G, and C main-belt asteroid classes ( *gray lines*) from Tholen & Barucci (1989).

meteorites, this band is attributed to charge transfer absorption in hydrated minerals. We infer that hydrated minerals are absent, either because KBOs are too cold to permit the aqueous alteration reactions needed for hydration, or because the compositions are dominated by complex organics.

We thank Pedro Lacerda, Bin Yang, and the anonymous referee for comments. This work was supported by a grant to D. J. from the National Science Foundation. N. P. acknowledges funding from the European Social Fund and FCT, Portugal (reference BPD18729-2004).

REFERENCES

Barucci, M. A., Doressoundiram, A., Tholen, D., Fulchignoni, M., & Lazzarin, M. 1999, Icarus, 142, 476
Burns, R. G. 1981, Annu. Rev. Earth Planet. Sci., 9, 345
Busarev, V. V., Dorofeeva, V. A., & Makalkin, A. B. 2003, Earth Moon Planets, 92, 345
Cayrel de Strobel, G. 1996, A&A Rev., 7, 243
Cloutis, E. A., Gaffey, M. J., & Moslow, T. F. 1994, Icarus, 107, 276
Cruikshank, D. P., Barucci, M. A., Emery, J. P., Fernández, Y. R., Grundy, W. M., Noll, K. S., & Stansberry, J. A. 2007, in Protostars and Planets V, ed. B. Reipurth, D. Jewitt, & K. Keil (Tucson: Univ. Arizona Press), 879
Davies, J. K., Green, S., McBride, N., Muzzerall, E., Tholen, D. J., Whiteley, R. J., Foster, M. J., & Hillier, J. K. 2000, Icarus, 146, 253
de Bergh, C., et al. 2004, A&A, 416, 791
Delsanti, A., Hainaut, O., Jourdeuil, E., Meech, K. J., Boehnhardt, H., & Barrera, L. 2004, A&A, 417, 1145
Doressoundiram, A., Peixinho, N., Doucet, C., Mousis, O., Barucci, M. A., Petit, J. M., & Veillet, C. 2005, Icarus, 174, 90
Efron, B., & Tibshirani, R. J. 1993, An Introduction to the Bootstrap (New York: Chapman & Hall)
Elliot, J. L., et al. 2005, AJ, 129, 1117
Feierberg, M. A., Lebofsky, L. A., & Tholen, D. J. 1985, Icarus, 63, 183
Gaffey, M. J., & McCord, T. B. 1978, Space Sci. Rev., 21, 555
Hainaut, O. R., & Delsanti, A. C. 2002, A&A, 389, 641
Hardorp, J. 1982, A&A, 105, 120
Hartmann, W. K., Tholen, D. J., Meech, K. J., & Cruikshank, D. P. 1990, Icarus, 83, 1
Jewitt, D. C. 2002, AJ, 123, 1039
Jewitt, D. C., & Luu, J. X. 1998, AJ, 115, 1667
———. 2001, AJ, 122, 2099
———. 2004, Nature, 432, 731
Landolt, A. U. 1992, AJ, 104, 340
Luu, J., & Jewitt, D. 1996, AJ, 112, 2310
Lykawka, P. S., & Mukai, T. 2005, Earth Moon Planets, 97, 107
———. 2007a, Icarus, 189, 213
———. 2007b, Icarus, in press
Merk, R., & Prialnik, D. 2006, Icarus, 183, 283
Oke, J. B., et al. 1995, PASP, 107, 375
Peixinho, N., Boehnhardt, H., Belskaya, I., Doressoundiram, A., Barucci, M. A., & Delsanti, A. 2004, Icarus, 170, 153
Rabinowitz, D. L., Schaefer, B. E., & Tourtellotte, S. W. 2007, AJ, 133, 26
Sheppard, S. S. 2007, AJ, 134, 787
Sheppard, S. S., & Jewitt, D. C. 2002, AJ, 124, 1757
Stephens, D. C., et al. 2003, Earth Moon Planets, 92, 251
Tegler, S. C., & Romanishin, W. 2000, Nature, 407, 979
Thébault, P., & Doressoundiram, A. 2003, Icarus, 162, 27
Tholen, D. J., & Barucci, M. A. 1989, in Asteroids II, ed. R. P. Binzel, T. Gehrels, & M. S. Matthews (Tucson: Univ. Arizona Press), 298
Trujillo, C. A., & Brown, M. E. 2002, ApJ, 566, L125
Tueg, H., & Schmidt-Kaler, T. 1982, A&A, 105, 400